CREEP CRACK GROWTH PROPERTIES OF WELDED JOINTS FOR HIGH Cr FERRITIC STEEL

M. Tabuchi[1], J. C. Ha[1] and A. T. Yokobori, Jr.[2]
[1] National Institute for Materials Science, Tsukuba, 305-0047 Japan
[2] Department of Nanomechanics, Tohoku University, Sendai, 980-8579 Japan

ABSTRACT

Type IV cracking in heat affected zone (HAZ) of weldment is a problem for advanced high Cr ferritic steels. It is important to predict initiation and growth of creep voids and cracks in weldment. Present paper clarified the Type IV crack initiation and growth properties in fine-grained HAZ of weldments for tungsten strengthened high Cr steel. On the basis of experimental results, the programs that simulate type IV fracture have been developed. The effect of HAZ width on vacancy diffusion and crack initiation was discussed.

1 INTRODUCTION

In consideration of reduction of CO_2 emissions and energy saving for thermal power plants, the steam pressure and temperature conditions of boiler components is tending to increase. Several types of 9-12% Cr boiler steels with high creep strength have been developed. P92 and P122 steels strengthened by tungsten addition are being now performed for application to ultra-supercritical (USC) power plants operating at around 898K. For these high Cr ferritic steels, the creep damages and cracks formed in HAZ of weldments, which is called Type IV crack, decrease the creep lives of welded joints [1, 2]. Poor creep strength of fine-grained HAZ structure is considered as the primary cause of Type IV fracture [3]. It is necessary to predict initiation and growth of creep voids and cracks in fine-grained HAZ of weldment.

Present paper has investigated the creep crack initiation and growth properties of P122 steel welded joints. The computational programs to simulate Type IV fracture have been developed. The effect of HAZ width on vacancy diffusion and crack initiation is discussed.

2 EXPERIMENTAL PROCEDURES

2.1 Material and welding

The material chosen for this study is an 11Cr-0.4Mo-2W-CuVNb steel (ASME P122) in the plate form of thickness 27mm. This plate was normalized at 1323K for 100 min and tempered at 1043K for 360 min. Welded joints were fabricated from the plates using multi-layer gas tungsten arc welding (GTAW) and laser beam welding (LBW) process. Welding consumable used for GTAW was matching filler wire developed recently for welding this class of steel. The width of HAZ was about 2.5mm for GTAW and 0.5mm for LBW.

2.2 Creep crack growth test

The tensile test and creep tests for weld metal, base metal, simulated coarse-grained and fine-grained HAZ were conducted at 923K using standard creep specimen with 6mm in

diameter and 30mm in gage length. The obtained material properties of Young's modulus, yield stress and Norton's law are shown in Table 1. The creep crack growth tests for base metal, welded joints and simulated fine-grained HAZ were conducted using CT specimen at 923K. The notch tip of welded joint specimen was located in HAZ. The fatigue pre-crack of 3mm in length was introduced at room temperature. After pre-cracking, 25% side-groove of thickness was machined. Creep crack length was measured by D.C. electrical potential method. The crack opening displacement was measured.

Table 1 Mechanical properties of P122 steel weldment at 923K.

	E (GPa)	σ_{ys} (MPa)	A ($MPa^{-n}h^{-1}$)	n
Weld metal	106	91	$2.45x10^{-36}$	14.8
Coarse-grained HAZ	99	135	$4.86x10^{-22}$	8.4
Fine-grained HAZ	77	82	$4.58x10^{-20}$	7.7
Base metal	103	104	$1.35x10^{-25}$	10.0

3 RESULTS AND DISCUSSIONS

3.1 Creep crack growth properties of welded joints

Figure 1 shows the example of creep crack propagation profile of welded joint specimen. Although the notch tip could not be machined in the center of HAZ in some cases, creep crack growth in fine-grained HAZ, i.e. type IV crack growth, was observed for all welded joint specimens. Figures 2 and 3 show the obtained creep crack growth curves for welded joints, base metal and simulated fine-grained HAZ tested at the load for initial K =18 and 16($MPa\,m^{1/2}$), respectively. For the welded joints, the incubation period, during which crack scarcely grows, exists and then crack grows rapidly in the accelerating stage.

The creep crack growth rate was evaluated by C^* parameter calculated as follows [4];

$$C^* = \frac{n}{n+1}\frac{P\,d\delta/dt}{B_N(W-a)}\left(\gamma-\frac{\beta}{n}\right) \qquad (1)$$

where, W is the specimen width, a is the crack length, P is the load, B_N is the net thickness, $d\delta/dt$ is the crack opening displacement rate, n is the creep exponent in Norton's law, and β and γ are the functions of a and W. The relations between creep crack growth rate (da/dt) *vs*. C^* parameter for welded joints, base metal and simulated HAZ are shown in Figure 4. There were not many differences in da/dt of welded joints and base metal for the present steel. The present highly strengthened high Cr steel showed higher da/dt than the low alloy 1CrMoV steel.

While the differences of da/dt was negligible, the crack growth life and crack initiation time of CT specimens was shorter for welded joints than for base metal in Figure 2and 3. From the present results, the prediction of crack initiation time was important for the evaluation of fracture life of the welded joints. Figure 5 shows the computed initial C^* line integral by FEM for plane stress condition using creep data of fine-grained HAZ and base metal in Table 1. Only the width of HAZ is different between GTAW, LBW and simulated HAZ for this computation. The experimental crack initiation time was plotted against computed C^*

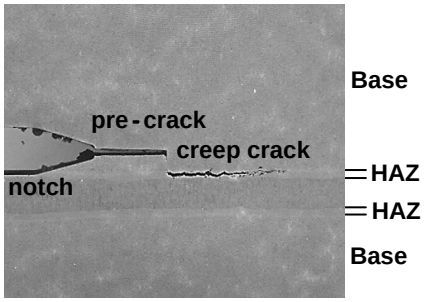

Figure 1: Type IV creep crack growth in LBW joint.

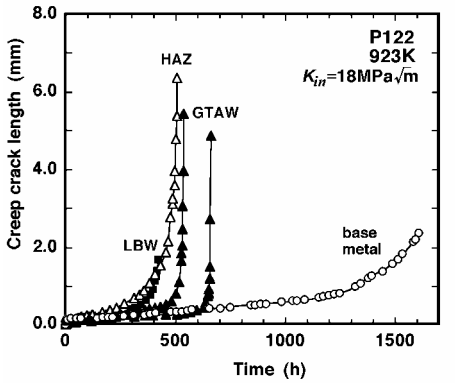

Figure 2: Creep crack length *vs*. time of base metal and welded joints for K_{in}=18(MPa m$^{1/2}$).

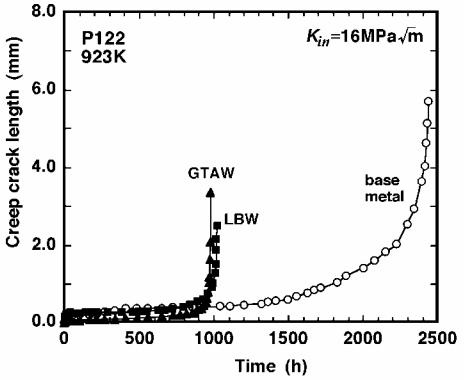

Figure 3: Creep crack length *vs*. time of base metal and welded joints for K_{in}=16(MPa m$^{1/2}$).

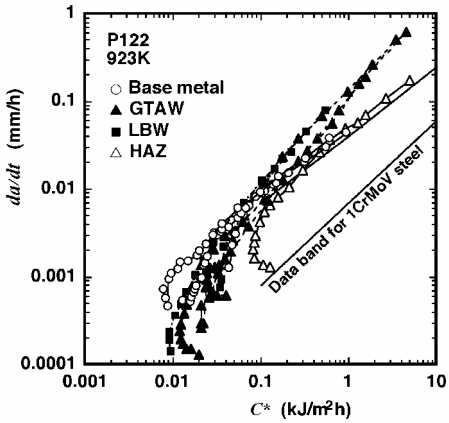

Figure 4: Creep crack growth rate *vs*. *C** for base metal and welded joints of P122 steel.

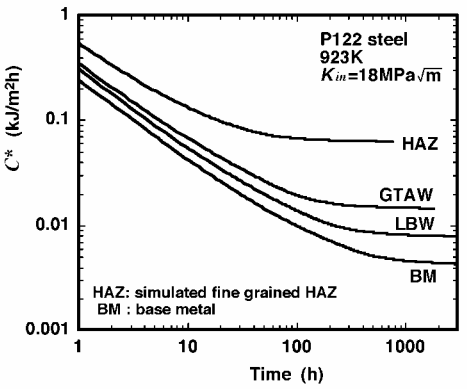

Figure 5: Computed initial *C** by FEM.

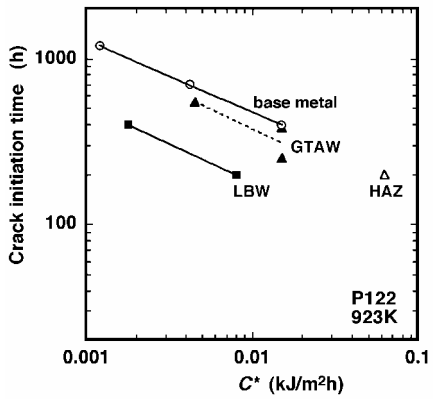

Figure 6: Crack initiation time *vs*. *C**.

value in Figure 6. Although the crack initiation time could be predicted from the initial C^* value [5], the effect of HAZ width on crack initiation, which seemed to be related to the mechanical constraint, was observed in the relations of Figure 6.

3.2 Simulation for Type IV creep crack growth

Based on the experimental results, we have conducted computational simulation for Type IV creep crack growth. The FEM analyses were conducted for the three-dimensional CT specimen model shown in Figure 7 using material constants in Table 1. Although the mesh size effect exists for crack growth simulation [6], here we use a comparatively coarse mesh due to many CPU times for three-dimensional simulation. The creep crack growth rate could be characterized by creep ductility ε_f^* [7, 8]. When the equivalent strain ahead of the crack tip reached to fracture strain, the coordinate of crack tip node was moved [9]. Figure 8 indicates the computed crack growth curves using ε_f^*=0.1. The creep crack growth behavior of GTAW joint and base metal could be simulated. Although decreasing HAZ width is predicted to increase the crack initiation and growth life from the computation of Figures 5 and 8, experimental results shows different tendency for LBW joint.

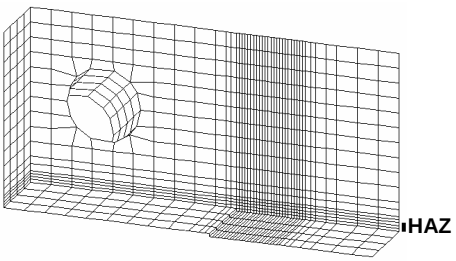

Figure 7: FE model of CT specimen.

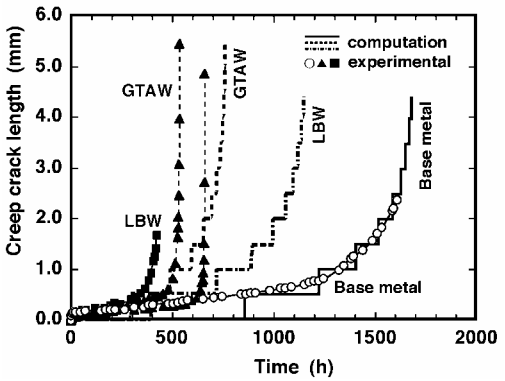

Figure 8: Computed creep crack growth against time for welded joint and base metal.

For the welded joints, the narrow HAZ with lower creep strength was mechanically constrained by base and weld metal with higher creep strength. The type IV crack in HAZ grew accompanying with creep voids ahead of the crack tip. It has been proposed that under creep conditions the diffusion of vacancies towards a crack or a void would contribute to crack growth [10]. Vacancy diffusion, void formation and crack propagation would be accelerated under multiaxial stress field. Here we evaluate the vacancy diffusion according to the following equation [11]:

$$\frac{\partial C}{\partial t} = \alpha_1 D \nabla^2 C + \alpha_2 \frac{D}{RT} \nabla C \nabla \nu \qquad (2)$$

$$\nu = -\sigma_p \Delta V \qquad (3)$$

where, C is the vacancy concentration, D is the diffusion coefficient, R is the gas constant,

T is the absolute temperature, σ_P is the hydrostatic stress, ΔV is the change of molar volume by vacancy diffusion and α_1 and α_2 are weight coefficient. The vacancy diffusion equation is solved for three-dimensional CT specimen model using the hydrostatic stress gradient $\nabla\sigma_p$ computed by FEM. The boundary conditions for vacancy diffusion analysis used here is $\partial C/\partial x = C\text{-}C_0$ at the crack tip and free for other specimen surfaces.

Figure 9 shows the computed result of changes in vacancy concentration ahead of the crack tip during creep using α_2/α_1=300, ΔV=2.0x10^{-6}(m^3/mol) and D=1.5x10^{-9}(m^2/s). The vacancy concentration increases faster for LBW than GTAW joint specimen. This consists with the experimental results that the crack initiation time is shorter for LBW than GTAW in Figure 6. This means that decreasing HAZ width can not prevent the void formation and Type IV fracture.

Because the vacancy concentration is related to creep damages, here we assume the following procedure. When the vacancy concentration increases, which means the formation of creep damages, the stiffness matrix [K] around the crack tip is decreased linearly dependent on the vacancy concentration. The computed result of Figure 10 shows that the crack initiation time and growth rate is accelerated by taking the damage formation due to vacancy diffusion into account. From these results, the creep void formation, which is affected by multiaxial stress condition, should be taken into consideration for life evaluation of welded joints.

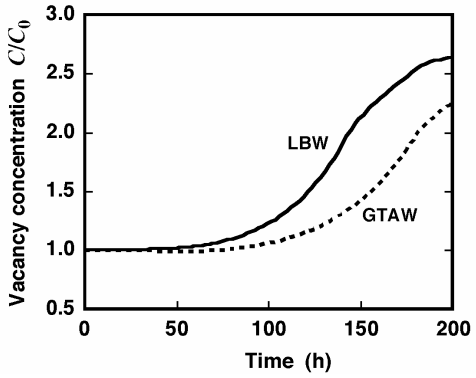

Figure 9: Changes of vacancy concentration ahead of the crack tip during creep.

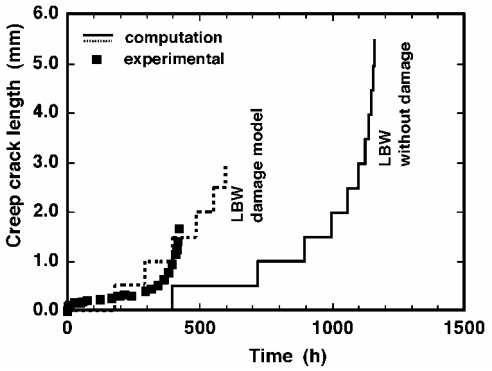

Figure 10: Creep crack growth curve taking the creep damages into consideration.

4 CONCLUSIONS

1. Creep crack growth tests of welded joints for 11Cr-0.4Mo-2W-CuVNb steel (P122) were conducted at 923K. Creep crack propagation in the fine-grained HAZ of weldment, i.e. Type IV crack, was observed for the present tests using CT specimen.
2. The differences in creep crack growth rate between welded joints and base metal was small for the present high strengthened steel, whereas the crack initiation time was shorter for welded joints than base metal.
3. Although the crack initiation time could be predicted from the initial C^* value computed by FEM, the effect of HAZ width on crack initiation, which was related to the mechanical constraint effect, was observed.

4. Three-dimensional programs, which analyze vacancy diffusion, damage development and crack growth under creep condition, have been developed in order to simulate Type IV fracture. Simulation can explain the experimental results of crack initiation and growth behavior.
5. The effect of multiaxial stress condition in HAZ of weldment on damage formation and crack initiation is considered to be important for life prediction of welded joints.

ACKNOWLEDGMENT

A part of this study was financially supported by the Budget for Nuclear Research of the Ministry of Education, Culture Sports, Science and Technology, based on the screening and counseling by Atomic Energy Commission.

REFERENCES

1. Bell K., Elevated temperature midlife weldment cracking (Type IV) - A review, TWI Report 597, Abington, Cambridge, 1997.
2. Masuyama F., Matsui M. and Komai N., Creep rupture behavior of advanced 9-12%Cr steel weldment, Key Engineering Materials, vol.171-174, pp.99-107, 2000.
3. Tabuchi M., Watanabe T., Kubo K., Matsui M., Kinugawa J. and Abe F., Creep crack growth behavior in the HAZ of weldments of W containing high Cr steel, Int. J. of Pressure Vessels & Piping, 78, pp.779-784, 2001.
4. Ernst H. A., Unified solution for *J* ranging continuously from pure bending to pure tension, ASTM STP 791, pp.I-499-519, 1983.
5. Webster G. A. and Ainsworth R. A., High Temperature Component Life Assessment, Chapman & Hall, London, pp.154-157, 1994.
6. Yatomi M., Nikbin K. M. and O'Dowd N. P., Creep crack growth prediction using a damage based approach, Int. J. of Pressure Vessels & Piping, 80, pp.573-583, 2003.
7. Nikbin K. M., Smith D. J. and Webster G. A., An engineering approach to the prediction of creep crack growth, Trans. ASME, J. Eng. Mater. Tech., 108, pp.186-191, 1986.
8. Tabuchi M., Ha J. C., Hongo H., Watanabe T., Yokobori Jr. A. T., Experimental and numerical study on the relationship between creep crack growth properties and fracture mechanisms, Metallurgical and Materials Transactions A, 35A, 2004 (in press).
9. Hsu T. R. and Zhai Z. H., A finite element algorithm for creep crack growth, Eng. Fract. Mech., 20, pp.521-533, 1984.
10. Leeuwen, H. P., The application of fracture mechanics to creep crack growth, Eng. Fract. Mech., 9, pp.951-974, 1977.
11. Yokobori Jr. A. T., Nemoto T., Satoh K. and Yamada T., Numerical analysis on hydrogen diffusion and concentration in solid with emission around the crack tip, Eng. Fract. Mech., 55, pp.47-60, 1996.